

Application Method of SfM/MVS Technique Combined with Point Cloud Data for Inspection of Steel Bridges

Ko Yamashita¹, Jun Kato¹

¹ Keisoku Research Consultant Co., Kyushu Division, 665-1 Fukuda, Higashi-ku, Hiroshima-shi, Hiroshima, Japan
email: k-yamashita@krcnet.co.jp, jun@krcnet.co.jp

ABSTRACT: The Structure from Motion/Multi-View Stereo (SfM/MVS) technique, which enables reconstruction of the three-dimensional shape of an object based on multi-view images, is a useful technique for inspection of infrastructure such as bridges in order to gain a comprehensive understanding of the state of damage. However, in SfM/MVS, the camera position and three-dimensional coordinates of the object are estimated based on feature points in images, making it difficult to apply this technique to steel structures, which have fewer feature points on surface textures due to coating. This paper presents a case in which SfM/MVS was successfully applied to a steel structure, specifically a steel bridge, by substituting the incomplete polygon model constructed in the conventional SfM/MVS process with a current-state CIM model created from existing drawings and point cloud data acquired with a terrestrial 3D laser scanner.

KEY WORDS: SfM/MVS; Terrestrial Laser Scanner; Point Cloud; Steel Bridge; Inspection; BIM/CIM.

1 INTRODUCTION

At present, aging of bridges in service and a shortage of inspection engineers have become problems in Japan [1], heightening the need for higher efficiency and labor-saving in bridge inspections. In this situation, preparation and wide use of Guidelines for Use of New Technologies [2], Delivery Manual for 3-Dimensional Deliverables [3] and other regulations are being promoted for image instrumentation technologies, including the Structure from Motion/Multi-View Stereo (SfM/MVS) technique [4], [5], which enables reconstruction of the three-dimensional shape of an object structure from images to gain an understanding of the state of damage, etc.

This study focuses on steel bridges as one type of bridge. As in other types of bridges, the problems associated with aging have also become apparent in steel bridges, as seen damage by corrosion of the steel materials [6]. However, it is sometimes difficult to apply the SfM/MVS technique to steel bridges since steel materials have fewer feature points, which are necessary for image processing, due to the uniform surface texture formed by coating film, and in such cases, reconstruction of the three-dimensional shape may be incomplete.

This paper examines the applicability of the SfM/MVS technique to steel bridges by using a method that utilizes a current-state CIM model (current-state CIM). This model was constructed by correcting existing drawings based on the current-state point cloud data (TLS point cloud) measured with terrestrial 3D laser scanners (TLS).

2 USE OF SfM/MVS AND POINT CLOUD DATA

2.1 Overview of SfM/MVS

SfM/MVS is a technique in which the three-dimensional geometry of an object is reconstructed from an image sequence (multi-view images) of the object by estimating the camera position and posture and the three-dimensional coordinates of the object by calculations based on feature points. Figure 1 is an image diagram of the reconstruction of a three-dimensional shape by SfM/MVS.

“Feature points” refer to points on the object appearing in the image that can be identified based on differences in color, brightness, etc., allowing its position to be determined. By detecting corresponding feature points between images, it becomes possible to estimate the relative camera position and posture with respect to the target structure, as well as the three-dimensional coordinates of each point. In general, the less uniform the surface texture of a structure, the greater the number of points detected as feature points. Accordingly, SfM/MVS technology can be effectively applied to structures with non-uniform surface textures and abundant feature points, such as concrete bridges.

2.2 Flow of Processing in SfM/MVS

The following describes the process of reconstructing the three-dimensional shape of an object by SfM/MVS and determining the three-dimensional location, size and other features of damage of the object structure. First, the point cloud data of the object structure is obtained by estimating the position and posture of the camera and the three-dimensional coordinates of the object structure based on the feature points described above. Next, a polygon model composed of surfaces is constructed based on the point cloud data, and a textured polygon model is obtained by applying textures sourced from photographic images onto the surface of that model. After this, it is possible to confirm the two-dimensional damage position and size by outputting orthoimages based on the textured polygon model. Figure 2 shows the general processing flow of SfM/MVS, including image acquisition.

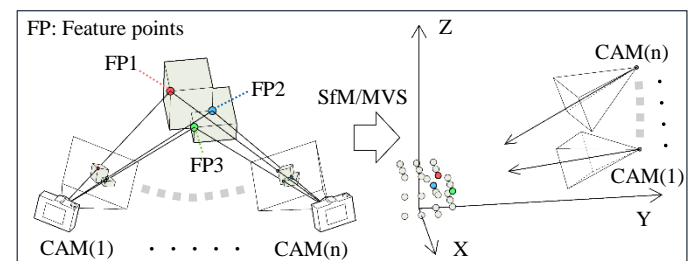


Figure 1. An image diagram of a three-dimensional shape reconstruction by SfM/MVS

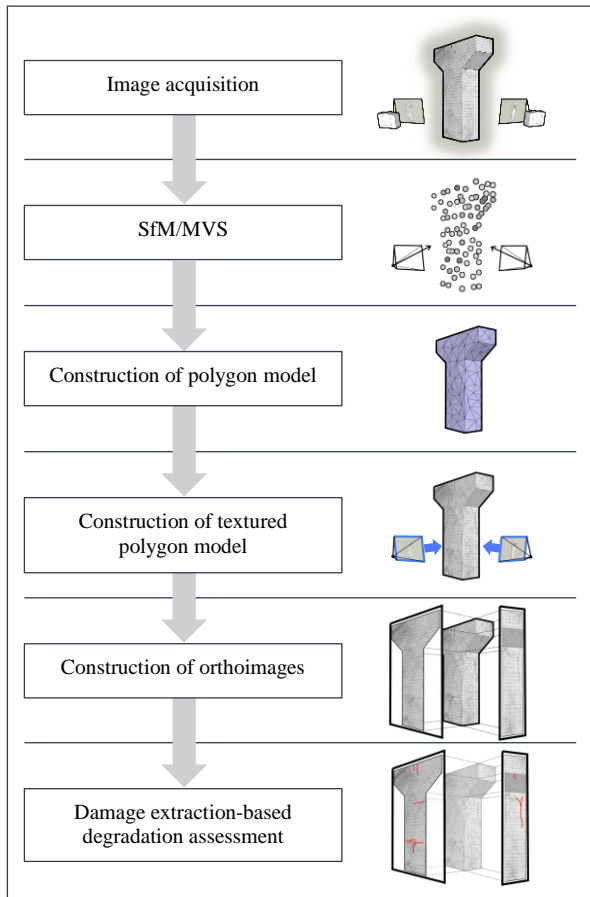


Figure 2. General Processing Flow for Applying SfM/MVS

2.3 Objects with Few Feature Points

The importance of feature points in SfM/MVS is as described above. However, when a paint film or other coating has been applied to the surface of the steel materials of a steel bridge, etc., the surface texture becomes uniform. This results in fewer points being detectable as feature points, making it difficult to apply SfM/MVS using general methods. Figure 3 shows a comparison of the detection status of corresponding feature points between objects with surface textures of varying uniformity. In the case of non-uniform surface texture, corresponding points are distributed across the entire surface. On the other hand, in the case of uniform surface texture, it is confirmed that corresponding points are not detected, except in distinctive areas such as corroded parts. Furthermore some manuals for general software products used in computational processing by SfM/MVS also recommend avoiding objects with a uniform texture or luster [7].

Figure 4 shows an example of constructing a point cloud data from SfM/MVS technique, targeting a steel bridge. In this example, there were many areas where the surface texture is uniform, and there were also areas where it was not possible to acquire a point cloud of the object structure at members that intrinsically have a flat surface due to the inadequate number of feature points. The inaccuracies in the shape of the polygon model and the improper placement of textures make it difficult to record the condition of damage of the entire object.

Figure 5 shows the processing flow for the problem that occur when SfM/MVS processing by the general technique is applied to an object with a uniform surface texture due to coating film.

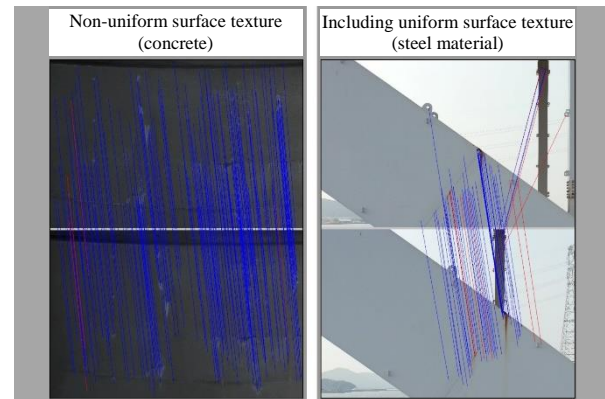


Figure 3. Comparison of the detection status of corresponding feature points

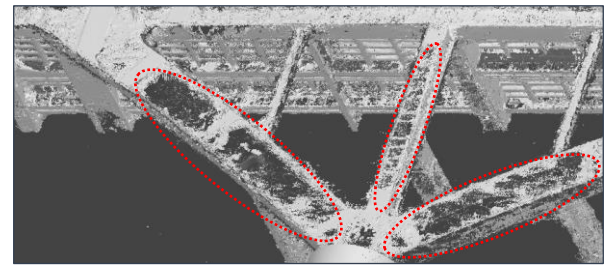


Figure 4. Point cloud where gaps occurred

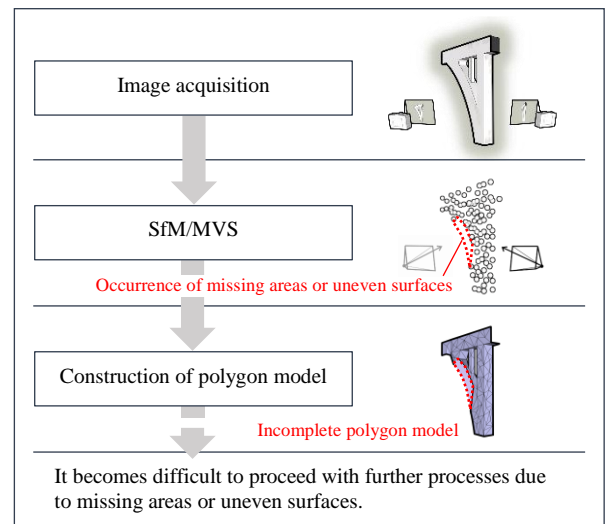


Figure 5. Problems in processing flow of SfM/MVS

2.4 SfM/MVS Combined with Measured Point Cloud Data

To solved the problems in application of SfM/MVS to steel bridges with few feature points, this paper examines a technique in which the object is measured with TLS, and the acquired measured point cloud data are used.

In this method, positions and posture of cameras, along with three-dimensional coordinates within the possible range, are first estimated using the conventional SfM/MVS approach.

Then, instead of the polygon model used in conventional methods, the current-state CIM, which reproduces the current shape of the object based on TLS point cloud and existing drawings, is utilized. Texture is projected onto this current-state CIM using camera images as sources, enabling the construction of textured models and orthoimages. Furthermore, even the incomplete polygon models created through conventional methods are used as a reference data for aligning the current-state CIM. UAV is employed for image acquisition, and during the SfM/MVS phase, GNSS data obtained during image acquisition is also used for analysis. This method is referred to as "SfM/MVS combined with TLS point cloud" and the processing flow is shown in Figure 6.

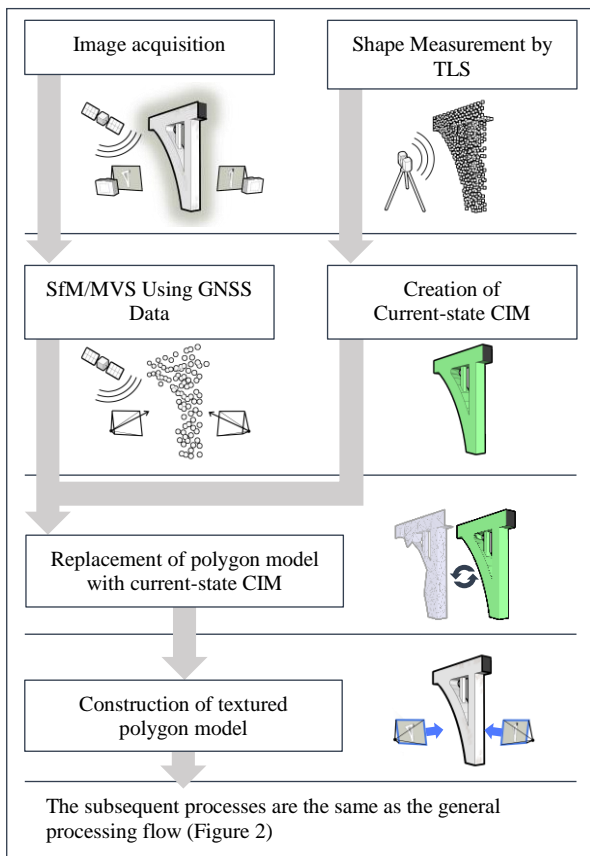


Figure 6. Processing flow of SfM/MVS combined with TLS point cloud

3 EXAMPLE OF APPLICATION TO AN ACTUAL STEEL BRIDGE

This chapter presents an example in which the proposed technique, SfM/MVS combined with TLS point cloud, was applied to an actual steel bridge. This verification is an attempt to apply SfM/MVS in work for investigation of the condition of corrosion and others of the steel materials of the object bridge.

3.1 Overview of Steel Bridge

The object bridge is a bridge with a total length of 651 meters, in which the main bridge section is a mid-height-deck arch Lohse structure as shown in Figure 7. The object range of the inspection was the steel parts between piers P5 and P8, as

shown in Figure 8. The bridge is constructed over the sea, and the distance between the revetments on the origin and terminus sides is approximately 450 meters. Owing to the water depth directly under the bridge between piers P5 and P7, it was impossible to enter this area on foot, but the area between piers P7 and P8 could be entered on foot at low tide. The specifications of the bridge are shown in Table 1. As can be seen in Figure 9, the steel materials in this object range have a uniform surface texture due to paint film.



Figure 7. Object bridge

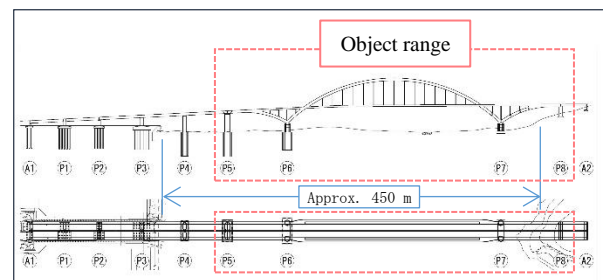


Figure 8. Object range

Table 1. Specifications of object bridge

Bridge name	Imari Bay Bridge
Date completed	2003
Location	Imari City, Saga Prefecture, Japan
Bridge length	651 m (over sea length: 420 m)
Width	Total width: 21.3 m
Space below girder	Height: 20.5 m, width: 200 m
Superstructure (main bridge part)	Steel 3-span continuous mid-height-deck Lohse bridge (70 m + 250 m + 70 m)



Figure 9. Steel with uniform surface texture

3.2 Equipment Used

Image acquisition was performed using two types of UAVs with an attached camera. A Matrice 300 RTK was mainly used, and a compact Skydio was used in some places. Table 2 shows the specifications of the UAVs and the attached cameras.

To acquire measured point cloud data on the current state of the object bridge, measurements were carried out with TLS. Two types were used in the measurements, a medium-range Focus S-350 (FARO) and a long-range SX10 (Trimble). Table 3 shows the specifications of the instruments.

The software used in image analyzing by SfM/MVS was Metashape Professional (Agisoft).

Table 2. Specifications of UAVs and camera






Manufacturer	DJI	
Type	Matrice 300 RTK	
Appearance		
Device	Item	Specification
Main unit	Dimensions (length x width x height)	810 x 670 x 430 mm
	Weight	6.3 kg (approx.)
	Flight time (max.)	55 min
	Auto flight function	Yes
	Cruising speed (max.)	17 m/s
	Max. operational wind speed	12 m/s
Name	Zenmuse P1 (mounted on Matrice 300 RTK)	
Appearance		
Dimensions	198 x 166 x 129 mm	
Weight	800 g (approx.)	
Sensor dimensions	35.9 x 24 mm	
Photo size	8 192 x 5 460 pixels	
Shutter speed	1/8 000 to 1 s	
Aperture range	F2.8 to F16	
ISO sensitivity	100 to 25 600	
Manufacturer	Skydio	
Type	Skydio 2+	
Appearance		
Device	Item	Specification
Main unit	Dimensions (length x width x height)	229 x 274 x 126 mm
	Weight	0.8 kg
	Flight time (max.)	27 min
	Auto flight function	Yes
	Cruising speed (max.)	58 km/h
	Max. operational wind speed	11.1 m/s
Mounted camera	Photo size	4 056 x 3 040 pixels
	Shutter speed	1/1 920 to 1 s
	Aperture value	F2.8
	ISO sensitivity	100 to 3 200

Table 3. Instrument specifications of TLS

Manufacturer	FARO	Trimble
Name	Focus S-350	SX10
Appearance		
Ranging method	Phase shift	Time-of-flight
Measurement distance	0.6 to 350 m	1 to 600 m
Measurement range	V:320° H:360°	V:150° H:360°
Laser class	Class 1	Class 1M
Scan speed	122 000 points/s	26 600 points/s
Accuracy	Three-dimensional positional accuracy	Distance measurement accuracy
	2mm@10m, 3.5+0.1mm/m@25m or more	2 mm + 1.5 ppm
Unit weight	4.2 kg	7.5 kg

3.3 Condition of Measurement

The condition of image acquisition by UAV is shown in Figure 10. To prevent UAV crash accidents, the UAVs were not flown directly over the bridge, and images were acquired from positions where visual confirmation of the UAV by the operator was possible. In acquiring the images of the underside of the girders between P7 and P8, we entered the riverbed area of P7 during low tide, and used the compact Skydio UAV to photograph the structure due to the limited space under the girders. To prevent image blurring, the shutter speed was set to approximately 1/1 000 s during photography, and continuous images were taken at intervals after adjusting the focus. The purpose of this work was to understand the positions and surface areas of corroded areas. Image acquisition was performed at a resolution of approximately 3 mm/pixel with a 45 megapixel camera (8 192 x 5 460 pixels), as this is adequate resolution for confirming corrosion and image processing, and SfM/MVS can be performed more easily with a wider field of view per image. Image acquisition by UAV was conducted over a 4-day period, and a total of 10 232 images were captured. Figure 11 shows the cross-sectional positions of image acquisition.

Figure 12 shows the condition of shape measurement of the object bridge by TLS. The Focus S-350 was used in measurements on the bridge. The inner surface shapes of the arch ribs and suspension members were measured. Additionally, given that the distance between the revetments at the bridge origin and terminus sides of the bridge is approximately 450 meters, the entire side elevation of the bridge was measured using the SX10 laser scanner, which enables long-distance measurement from both revetments. Figure 13 shows the measurements positions of the two TLS.



Figure 10. Condition of image acquisition by UAV

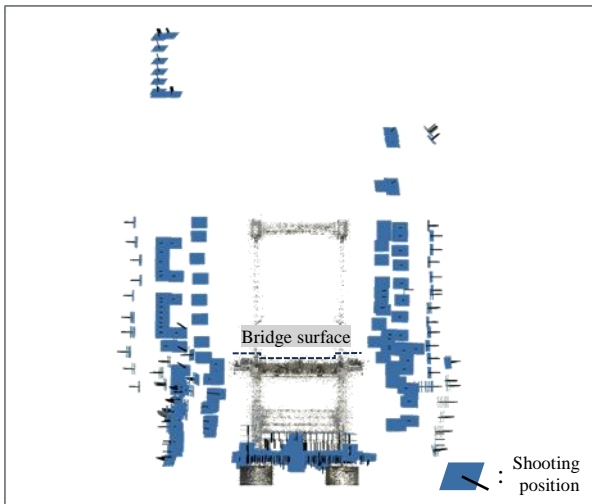


Figure 11. Positions of image acquisition by UAV (section view)



Figure 12. Condition of measurements by TLS (left: from revetment, right: on bridge)



Figure 13. Positions of measurements by TLS (Created using aerial photographs (by the Geospatial Information Authority of Japan))

3.4 Measurement Results

The TLS point cloud of entire bridge shape is shown in Figure 14. By precisely aligning the point cloud data measured from the various positions, the point cloud data representing the entire bridge shape were obtained.

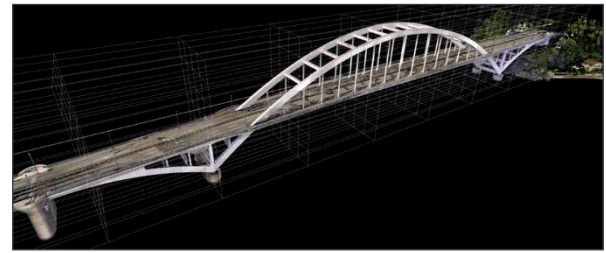


Figure 14. TLS point cloud of entire bridge shape

3.5 Creation of Current-state CIM Based on TLS Point Cloud

When the TLS point cloud was superimposed on existing drawings data, as shown in Figure 15, deviations were observed in the lateral shape of the arch rib members. Therefore, the linear data of existing drawings were corrected in accordance with the geometry of the TLS point cloud. The condition of correction of the drawing data is shown in Figure 16.

Next, based on the corrected drawing data, a current-state CIM of the bridge was created. The condition of creation of this current-state CIM is shown in Figure 17. The required level of performance for reproducing CIM models, based on their intended use, is defined as "Level of Detail (LOD)" in the Guidelines for Introduction of CIM [8], [9] issued by Japan's Ministry of Land, Infrastructure, Transport and Tourism. Excerpts of the definitions of each specified level of detail are shown in Table 4. In the range where point cloud data were acquired for steel materials, an LOD of approximately 300 was used, as it was possible to understand the external shape. However, in the range where point cloud data could not be acquired, for example, on the underside of girders, modelling was performed using LODs of 200 to 300, referring to the data in existing drawings, etc. The created current-state CIM created is shown in Figure 18.



Figure 15. Overlay of measured cloud point data and drawing data

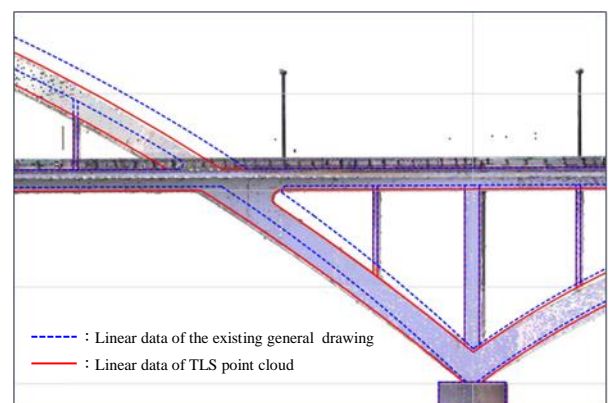


Figure 16. Correction of drawing data

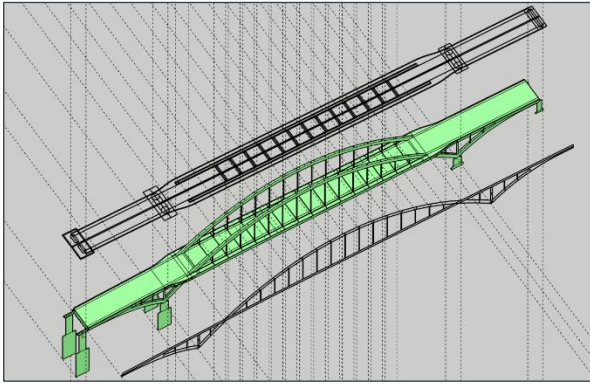


Figure 17. Creation of current-state CIM

Table 4. Definitions of levels of detail (LOD)

LOD	Common definition
100	Model showing the position of the object by symbols, lines or simple shapes.
200	Model with sufficient detail to understand the structural type. Cuts and fills are represented by standard transects, or in sufficient detail to sweep the standard transects of each structure in the general drawing in the object range.
300	Model accurately representing the external geometry of the object, with the exception of ancillary works and other detailed structures and the structure of connecting parts.
400	In addition to the requirements of LOD 300, accurate modeling is performed, including ancillary works, connecting structures and other detailed structures and the arrangement of reinforcing materials.
500	Model representing the actual geometry of the object.

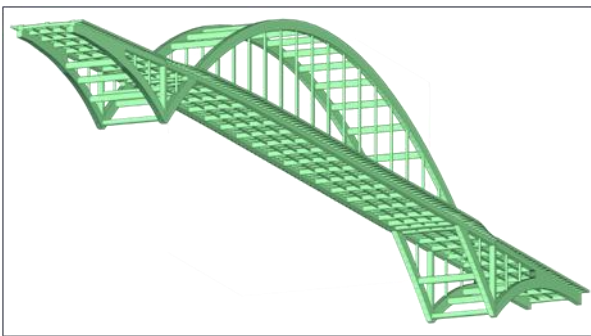


Figure 18. Created current-state CIM

3.6 SfM/MVS combined with TLS point cloud Application Process and Results

First, sparse point cloud data of the object bridge were obtained using location information from the GNSS data of UAV-captured images and camera posture information derived from SfM analysis. The results are shown in Figure 19.

Subsequently, for the dense point cloud data obtained through MVS analysis, a color map was created based on the number of depth maps used to generate each point cloud, as shown in Figure 20. A depth map is data that indicates the distance from the camera to each pixel in an image, and it is generally determined that the more depth maps used in the point cloud generation process, the higher the reliability of the

point cloud data. The number of point cloud for each confidence level is shown in Table 5. As shown in Figure 20, while a large number of depth maps were used in some areas, a decrease in the number of depth maps used was observed near areas with missing point cloud.

In the following step, in order to create textures based on camera images and construct a textured polygon model for the created current-state CIM, the current-state CIM and the cameras must be in the correct positional relationship. Therefore, to align the current-state CIM, a polygon model was first created based on the point cloud obtained through conventional SfM/MVS. As shown in Figure 21, although this model itself was an incomplete polygon model with missing areas and unevenness in originally flat sections, the point cloud derived from SfM/MVS with a confidence level of 10 or higher were superimposed on the TLS point cloud, and their differences were examined, as shown in Figure 22 and Table 6. As a result, 57.34% of the point cloud fell within a difference of 0.15 m and was distributed across the entire bridge. Note that 27.86% of the point cloud showed a difference of 0.3 m or more, which is thought to be primarily due to differences calculated at the lower parts of the girders where sufficient measurement using TLS was not possible.

Based on these results, the overall shape of the bridge and areas with high confidence were deemed to have a sufficient level of precision to serve as data indicating the positional relationship between the bridge and the camera. Therefore, the constructed incomplete polygon model was used as a reference for aligning the current-state CIM.

Subsequently, the aligned current-state CIM was imported into the SfM/MVS software, enabling the creation of an accurate textured polygon model. Figure 23 shows the data of the SfM/MVS application process using the current-state CIM, and Figure 24 shows the textured model created by this process. In addition to being able to confirm damage such as corrosion on the textured model, it became possible to output orthoimages, as shown in Figure 25, and accurately record the location, size, and other details of the damage by overlaying the orthoimages with drawings. Furthermore, the visualization of damaged areas using the 3D model enabled desk-based assessments of deterioration, as shown in Figure 26.

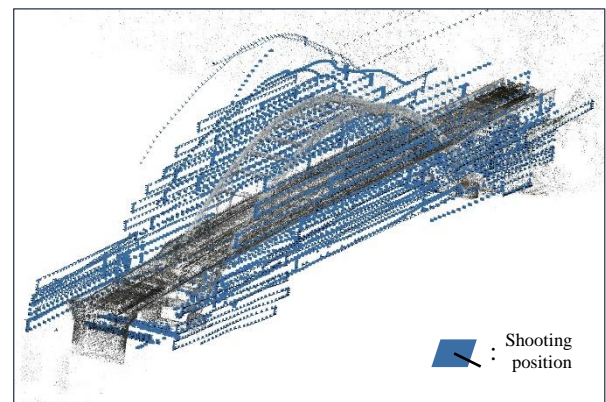


Figure 19. Estimation of camera position based on GNSS coordinate information

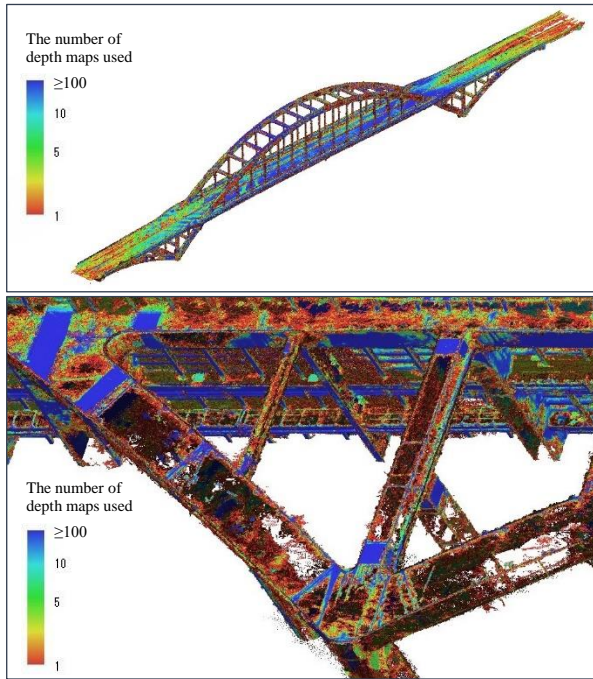


Figure 20. The confidence map of point cloud generated by SfM/MVS

Table 5. Number of point cloud for each confidence level

Confidence level (number of depth maps used)	Number and proportion of point cloud
1 to 4	150,509,599 points (54.38 %)
5 to 9	50,222,768 points (18.14 %)
10 to 99	75,733,315 points (27.36 %)
100 or more	330,028 points (0.12 %)

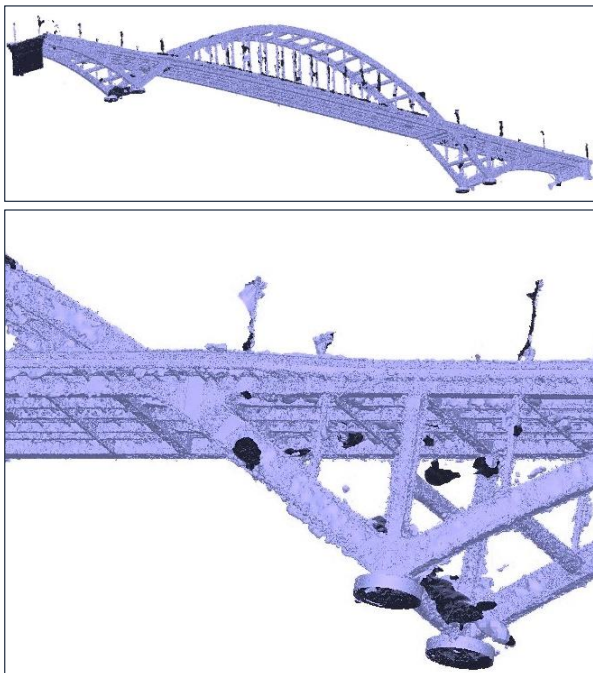


Figure 21. Results of SfM/MVS processing by the conventional technique

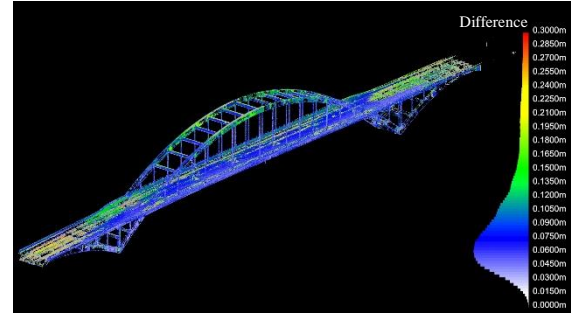


Figure 22. The difference color map between point SfM/MVS point cloud (high-confidence area) and TLS point cloud

Table 6. The difference verification results between point cloud generated by SfM/MVS (high-confidence area) and TLS

Statistics	Range of color map	0.000 m to 0.300 m
	Total point cloud (Sampled with an average point spacing of 10 cm)	2,819,768 points
	Point count in range	2,034,179 points
	Mean distance from base surfaces	0.1056 m (0.0655 std dev.)
Point Distribution	0.000 m to 0.075 m	836,198 points (29.66 %)
	0.075 m to 0.150 m	780,498 points (27.68 %)
	0.150 m to 0.225 m	247,846 points (8.79 %)
	0.225 m to 0.300 m	169,637 points (6.02 %)
	0.300 m or more	785,589 points (27.86 %)

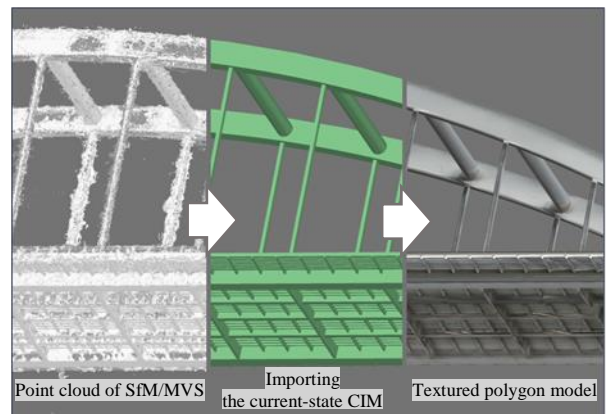


Figure 23. The application process of current-state CIM



Figure 24. Created textured polygon model

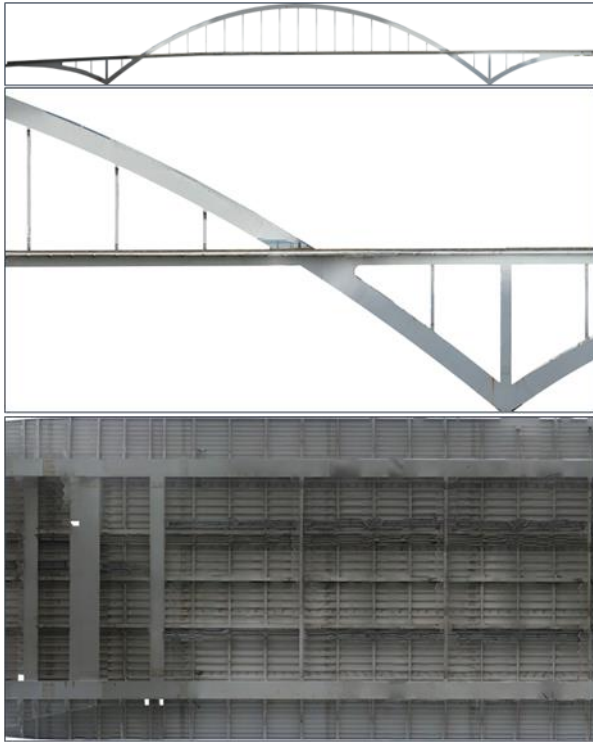


Figure 25. Examples of created orthoimages

(Top and middle images: bridge side view, bottom image: underside of the girder)

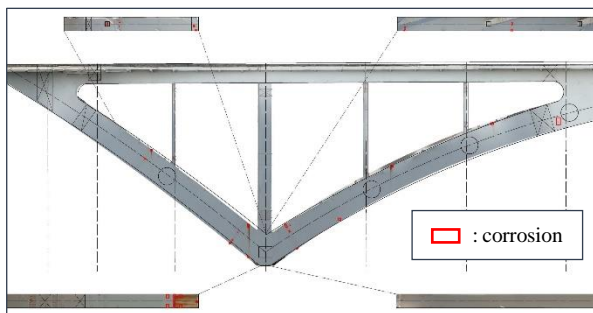


Figure 26. Example of a damage map created based on orthoimages

3.7 Issues

Four points may be mentioned as issues in the SfM/MVS combined technique using measured point cloud data described in this paper: i), Increase in costs associated with the construction of the current-state CIM, ii) Accuracy and level of detail of the current-state CIM, iii) Accuracy of alignment of the current-state CIM and camera positions and iv) Applicability of SfM/MVS to more difficult cases.

i) Cost incurred in construction of the current-state CIM

Compared to conventional SfM/MVS, the measurement of point cloud data aimed at understanding the current-state shape, the modification of drawing data to match the actual shape, and the creation of the current-state CIM lead to an increase in costs and workflow. It is necessary to plan accordingly to ensure efficient and sufficient data acquisition, based on the purpose of applying SfM/MVS techniques. This involves selecting appropriate equipment, preparing a measurement plan, and

considering factors such as the level of detail (LOD) of the 3D model, as described later.

ii) Accuracy and level of detail of the current-state CIM

The current-state CIM prepared in the proposed method will contain errors due to measurement accuracy, accuracy during model preparation and the setting of LOD. As the error in shape estimation increases, the accuracy of the positional relationship of the model and the cameras will decrease, leading to decreased quality of the textures to be projected. In actuality, even in the case described in this paper, it was confirmed that due to the difficulty in capturing detailed geometry using TLS, the quality of textures decreased in parts on the underside of the girders, where the level of detail of the current-state CIM was low, compared to other areas.

iii) Accuracy of alignment of the current-state CIM and camera positions

The point cloud obtained through conventional SfM/MVS processing was confirmed to be usable as reference data for alignment based on comparative verification with the TLS point cloud. Using the constructed incomplete polygon model as a reference, the alignment between the current-state CIM and the camera was performed. On the other hand, to ensure the accuracy and reproducibility of alignment, it is desirable to manage coordinates on public coordinate systems. This can be achieved by setting up multiple ground control points during UAV imaging and TLS measurements, and performing processes such as aligning the control points placed on the current-state CIM based on the TLS point cloud with the control point coordinates calculated by SfM/MVS.

iv) Applicability of SfM/MVS to more difficult cases

In the example described in this case, it was possible to estimate the camera positions by applying conventional SfM/MVS and perform polygon modeling, although incomplete. The factors in this successful result are thought to include the fact that image acquisition was performed by setting the angle of view to capture a wide range in photography by the UAVs, and corroded parts and fine irregularities on members could be detected and used as feature points. Thus, there is a possibility that the technique described in this paper may be inadequate for steel bridges and other structures with uniform surface textures or flat shapes over larger areas. Therefore, going forward, it will be necessary to consider combining SfM/MVS with other 3D model acquisition techniques, including improvements to the methods discussed in this paper.

4 CONCLUSION

As a technique for applying SfM/MVS to steel bridges, in which the steel materials have a uniform surface texture as a result of coating film, this paper examined a processing flow for projecting textures from camera images on a current-state CIM model based on measured point cloud data obtained with terrestrial 3D laser scanners. The technique was also verified at an actual bridge. Although the quality of textures differed depending on the accuracy and level of detail (LOD) of the current-state CIM model, the possibility of constructing a textured model and orthoimages with sufficient quality to identify overall damage could be confirmed.

On the other hand, various issues for application of the SfM/MVS technique verified in this paper may be mentioned.

These include the cost of creating the current-state CIM model, the accuracy and LOD of the model, the accuracy of alignment, and the applicability of the proposed technique to more difficult object structures. To overcome these problems, it will be necessary to plan methods corresponding to the purpose of applying SfM/MVS, the geometry of the object structure, and the surrounding environment. In the case described in this paper, the current-state CIM model was prepared based on existing drawings and the measured point cloud data of the current shape of the structure. In the future, the application of BIM/CIM, which has been actively promoted in recent years, may make it possible to substitute the current-state CIM with BIM/CIM models constructed at stages prior to inspections.

As future work on SfM/MVS application techniques, the authors intend to improve the accuracy and expand the range of application of the SfM/MVS technique, and study approaches for realizing higher efficiency and labor-saving in bridge inspections of steel bridges.

REFERENCES

- [1] Ministry of Land, Infrastructure, Transport and Tourism (MLIT), Efforts for Aging Countermeasures, pp. 1–2, Japan, 2022, [Online], Available: <https://www.mlit.go.jp/road/sisaku/yobohozen/torikumi.pdf>
- [2] Ministry of Land, Infrastructure, Transport and Tourism (MLIT), Guidelines for Using New Technologies (Draft), Japan, 2019, [Online], Available: https://www.mlit.go.jp/road/sisaku/yobohozen/tenken/yobo5_1.pdf.
- [3] Ministry of Land, Infrastructure, Transport and Tourism (MLIT), 3D Product Delivery Manual Using Inspection Support Technologies (Image Measurement Technologies) [Bridge Edition] (Draft), Japan, 2023, [Online], Available: <https://www.mlit.go.jp/tec/constplan/content/001612927.pdf>.
- [4] K. Oda, Explanation: Structure from Motion (SfM) – Part 1: Overview of SfM and Bundle Adjustment, Photogrammetry and Remote Sensing, vol. 55, no. 3, pp. 206–209, Japan, 2016.
- [5] T. Fuse, Explanation: Structure from Motion (SfM) – Part 2: SfM and Multi-View Stereo, Photogrammetry and Remote Sensing, vol. 55, no. 4, pp. 259–262, Japan, 2016.
- [6] National Institute for Land and Infrastructure Management (NILIM), A Study on the Advancement of Environmental Evaluation Methods for Weathering Steel Bridges (I) — Examination of Environmental Evaluation Methods for Weathering Steel Materials —, NILIM Material No. 777, Japan, 2014.
- [7] Agisoft LLC, Agisoft Metashape User Manual, Professional Edition, ver. 2.2, pp. 9, 2025.
- [8] Ministry of Land, Infrastructure, Transport and Tourism (MLIT), CIM Introduction Guidelines (Draft) Part 1: Common Edition, Reference Materials, pp. 20–21, Japan, 2020, [Online], Available: <https://www.mlit.go.jp/tec/content/001334802.pdf>.
- [9] Ministry of Land, Infrastructure, Transport and Tourism (MLIT), CIM Introduction Guidelines (Draft) Part 5: Bridge Edition, pp. 12, Japan, 2020, [Online], Available: <https://www.mlit.go.jp/tec/content/001334799.pdf>.